Radiative Recombination and Photoionization for Tungsten Ions in Plasmas

M. B. Trzhaskovskaya
Department of Theoretical Physics
Petersburg Nuclear Physics Institute, Gatchina 188300, Russia

V. K. Nikulin
Division of Plasma Physics, Atomic Physics, and Astrophysics
A.F.Ioffe Physical-Technical Institute, St.Petersburg 194021, Russia

Research Co-ordination Meeting on CRP
"Spectroscopic and Collisional Data for Tungsten in Plasma from 1 eV to 20 keV"

IAEA, Vienna, Austria, 13–15 December, 2010

Introduction

Radiative recombination (RR) is one of the important mechanisms influencing the equilibria and the thermal balance of fusion plasmas. In parallel with the commonly used plasma diagnostics adopting theoretical data for radiative recombination and for the inverse process photoionization, new active spectroscopy diagnostics of highly-charged tungsten ions based on observation of x-ray radiation has been proposed at the Berlin EBIT [C. Biedermann *et al.*, Phys.Scr.T **134**, 014026 (2009)]. The main special feature of the diagnostics is that the signature of RR appears in the x-ray spectrum as distinct lines. To obtain the relative charge state abundance, a fit of theoretical intensities for relevant ion states to experimental RR spectrum have to be performed, that is, the accurate values of RR cross sections are required.

In the framework of the previous Coordinated Research Project **"Atomic data for heavy element impurities in fusion reactors" (2005-2009)**, we elaborated a new unified database involving partial and total RR cross sections (RRCS) and partial photoionization cross sections (PCS) for around 90 ions of 16 elements, including ten tungsten ions as well as RR rate coefficients (RR rates) for nine tungsten ions.

Table 1. Charges of recombining ions

Config.	Si	P	S	Cl	Ar	K	Ca	Ti	Cr	Fe	Ni	Cu	Kr	Mo	Xe	W
bare nucl.	14	15	16	17	18	19	20	22	24	26	28	29	36	42	54	74
H-like	13	14	15	16	17	18	19	21	23	25	27	28	35	41	53	73
He-like	12	13	14	15	16	17	18	20	22	24	26	27	34	40	52	72
Be-like		11	12			15	16									70
Ne-like	4	5	6	7	8	9	10	12	14	16	18	19	26	32	44	64
Ar-like							2	4	6	8	10	11	18	24	36	56
"Ni-like"													8	14	26	46
Kr-like														6	18	38
Pd-like															8	28
"Er-like"																6

Note: the "Ni-like" configuration is $[\mathrm{Ar}]3d^4_{3/2}3d^6_{5/2}$ instead of the standard one $4s^2 3d^4_{3/2}3d^4_{5/2}$; the "Er-like" configuration is $[\mathrm{Xe}]4f^6_{5/2}4f^8_{7/2}$ instead of $6s^2 4f^6_{5/2}4f^6_{7/2}$.

PCS and RRCS were obtained in the kinetic electron energy range **1 eV - 50 keV**. Partial PCS were fitted by an analytical expression involving five fit parameters. RR rates were computed in the wide temperature range **10^3 K - 10^{10} K**.

The calculations are based on the fully relativistic treatment of the processes. The Dirac-Fock (DF) method is used. All significant multipoles of the radiative field are taken into account. For the first time, the relativistic RR rates are found using relativistic RRCS provided the continuum electron velocity is described by the relativistic Maxwell-Jüttner distribution. The calculations were carried out with **our computer code package RAINE**.

The data were published in **5 papers** [M.B. Trzhaskovskaya, V.K. Nikulin, R.E.H. Clark, Phys.Rev.E **78**, 035401 (R) (2008); ADNDT **94** 71 (2008); ADNDT **95**, 987 (2009); ADNDT **96**, 1 (2010); ADNDT (in press) (2010);] and in **5 Reports of Petersburg Nuclear Physic Institute** and are available in "IAEA Atomic and Molecular Database" [http://www-amdis.iaea.org/ALADDIN].

1. Basic formulas
2. Exchange effects
3. Relativistic and non-dipole effects
4. Comparison of present calculations with previous results
5. Total radiative recombination cross sections
6. Fitting partial photoionization cross sections
7. Conclusions
8. Proposed researches

1. Basic formulas

Relativistic expressions for PCS in the i-th subshell are written as follows :

$$\sigma_{\rm ph}^{(i)} = \frac{4\pi^2\alpha}{k(2j_i+1)}\sum_L\sum_\kappa\Big[(2L+1)Q^2_{LL}(\kappa)+LQ^2_{L+1L}(\kappa) \quad (1)$$

$$+ (L+1)Q^2_{L-1L}(\kappa)-2\sqrt{L(L+1)}\,Q_{L-1L}(\kappa)Q_{L+1L}(\kappa)\Big] .$$

Here k is the photon energy, L is the multipolarity of the radiative field, the relativistic quantum number $\kappa=(\ell-j)(2j+1)$, j and ℓ are the total and orbital momentum of the electron, and α is the fine structure constant, relativistic units ($\hbar=m_0=c=1$) are used. The reduced matrix element $Q_{\Lambda L}(\kappa)$ has the form

$$Q_{\Lambda L}(\kappa) = \left[(2\bar{\ell}+1)(2\ell_i+1)/(2\Lambda+1)\right]^{1/2} C^{\Lambda 0}_{\bar{\ell}0\ell_i0}\,\mathcal{A}\begin{pmatrix}\bar{\ell} & 1/2 & j\\ \ell_i & 1/2 & j_i\\ \Lambda & 1 & L\end{pmatrix} R_{1\Lambda} \quad (2)$$

$$+ \left[(2\ell+1)(2\bar{\ell}_i+1)/(2\Lambda+1)\right]^{1/2} C^{\Lambda 0}_{\ell0\bar{\ell}_i0}\,\mathcal{A}\begin{pmatrix}\ell & 1/2 & j\\ \bar{\ell}_i & 1/2 & j_i\\ \Lambda & 1 & L\end{pmatrix} R_{2\Lambda} ,$$

where $\bar{\ell} = 2j - \ell$, $C^{\Lambda 0}_{\ell_1 0 \ell_2 0}$ is the Clebsch–Gordan coefficient, $\mathcal{A} \begin{pmatrix} \ell_1 & 1/2 & j_1 \\ \ell_2 & 1/2 & j_2 \\ \Lambda & 1 & L \end{pmatrix}$ is the recoupling coefficient for the four angular momenta ,$R_{1\Lambda}$ and $R_{2\Lambda}$ are radial integrals

$$R_{1\Lambda} = \int_0^\infty G_i(r) F(r) j_\Lambda(kr) dr \ , \tag{3}$$

$$R_{2\Lambda} = \int_0^\infty G(r) F_i(r) j_\Lambda(kr) dr \ .$$

Here $G(r)$ and $F(r)$ are the large and small components of the Dirac electron wave function multiplied by r, $j_\Lambda(kr)$ is the spherical Bessel function of the Λ-th order. The bound (subscript i) and continuum (no subscript) wave functions are calculated in the DF field of the corresponding ions with $N + 1$ and N electrons, respectively.

The partial RRCS for the recombining ion with N electrons when a free electron is captured to the i-th subshell can be expressed in terms of PCS for the corresponding recombined ion with $N+1$ electrons as follows

$$\sigma_{\rm rr}^{(i)} = A\, q^{(i)}\, \sigma_{\rm ph}^{(i)} \,. \tag{4}$$

Here $q^{(i)}$ is the number of vacancies in the i-th subshell prior to recombination and A is the transformation coefficient which can be derived from the principle of the detailed balance. The relativistic equation for the coefficient has the form

$$A_{\rm rel} = \frac{k^2}{2m_0c^2E_k + E_k^2} \,. \tag{5}$$

2. Exchange effects

As distinct from the widely-used Dirac-Slater (DS) method with the approximate exchange, in the DF method, the electron exchange is included exactly both between bound electrons and between bound and free electrons. PCS and RRCS obtained with the **DF and DS** methods may **considerably differ**, especially **for many-electron ions and at low electron energies**.

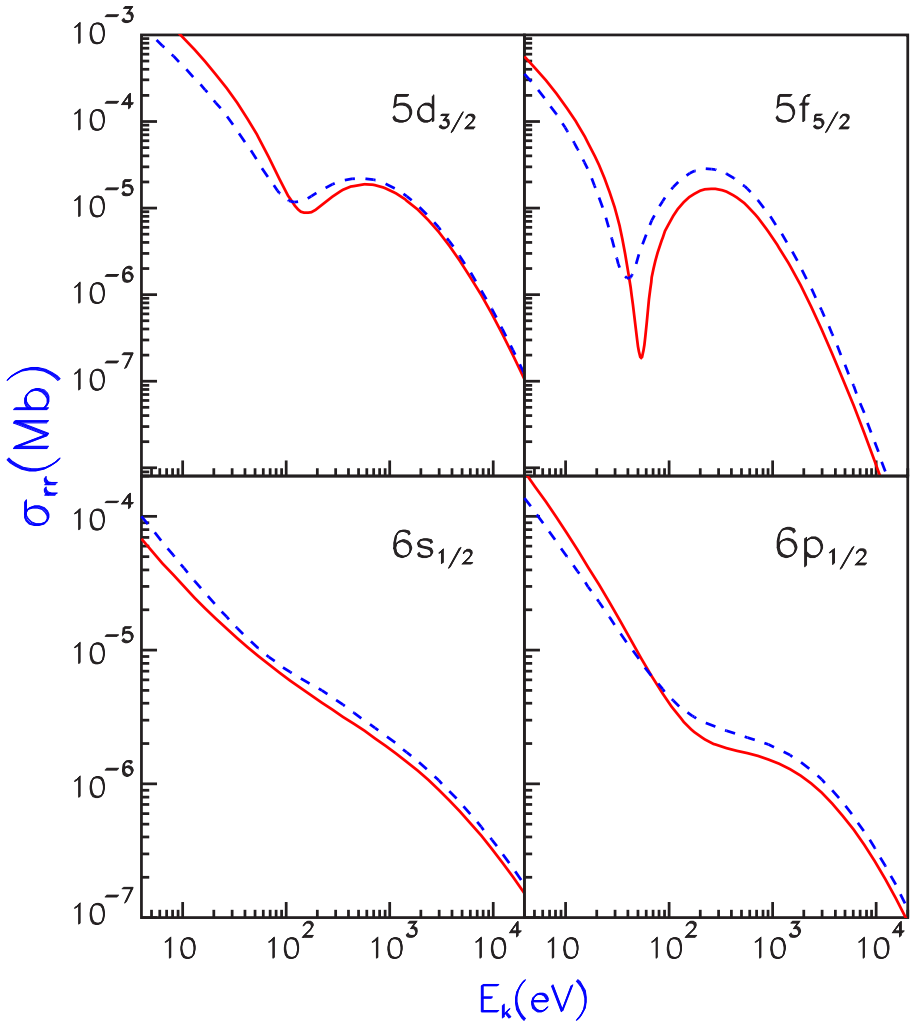

Figure 1: Partial RRCS for recombination of the W^{6+} ion with the $5d_{3/2}, 5f_{5/2}, 6s_{1/2}$, and $6p_{1/2}$ electrons. Solid red, DF calculation; dashed blue, DS calculation.

Table 2. Difference $\Delta_{\rm DS} = (\sigma_{\rm rr}^{\rm DS} - \sigma_{\rm rr}^{\rm DF})/\sigma_{\rm rr}^{\rm DF}$ (in %) between partial RRCS for the W^{6+} ion calculated by the use of the DF and DS methods.

E_k, eV	$5d_{3/2}$	$5f_{5/2}$	$6s_{1/2}$	$6p_{1/2}$
4	-53	81	46	-36
10	-53	45	37	-33
54	-48	1780	15	-7
109	-6	116	16	156
1153	13	61	19	28
15464	14	67	16	25
31391	13	71	14	23
50327	13	71	14	23

As is seen, the difference $\Delta_{\rm DS}$ is important at low electron energies but is considerable at higher energies as well. For example, in the energy range 1 keV $\lesssim E_k \lesssim$ 50 keV, the difference between the DS and DF results is also large — up to 71% and kept approximately constant value. Due to the large difference in RRCS and in PCS as well, the more accurate DF model should be preferred.

3. Relativistic and non-dipole effects

As is well known, the relativistic and non-dipole (multipole) effects are of great importance in consideration of photoionization and RR **for heavy and highly-charged ions at enough high electron energies**. In particular, Ichihara and Eichler [A. Ichihara, J. Eichler, ADNDT **74**, 1 (2000)] noted that the difference between the relativistic calculation of RRCS with regard to all multipoles and the non-relativistic calculation within the dipole approximation (NRD) for the $\boldsymbol{1s, 2p}$ and $\boldsymbol{3d}$ shells of the uranium ion **reaches 18%** even at electron energy as low as $\boldsymbol{E_k}$**=10 eV**, by a factor of 2 at $\boldsymbol{E_k}$=100 keV, and exceeds an order of magnitude at $\boldsymbol{E_k}$=1000 keV. Nevertheless, the multipole and relativistic effects are often neglected in plasma calculations.

In our calculations, relativistic and multipole effects are taken into consideration. Moreover, a new fully relativistic formula for the RR and radiated power loss (RPL) rate coefficients was obtained by a consistent way, that is, firstly, using the relativistic expression for PCS; secondly, the relativistic expression for the transformation coefficient from PCS to RRCS; and, finally, the relativistic Maxwellian distribution of continuum electrons instead of the non-relativistic distribution adopted in all previous calculations.

The relativistic RR rate coefficient $\boldsymbol{\alpha_{rel}^{(n\kappa)}(T)}$ can be found using the thermal average

over the fully relativistic RRCS, the continuum electron velocity being described by the relativistic Maxwell-Jüttner distribution function $f(E)$ normalized to unity [F.Jüttner, Ann. Phys. (Leipzig) **34**, 856 (1911); M. Alexanian, Phys. Rev. **165**, 253 (1968)].

$$f(E)dE = \frac{E(E^2-1)^{1/2}}{\theta e^{1/\theta} K_2(1/\theta)} \times e^{-(E-1)/\theta} dE. \quad (6)$$

Here E is the total electron energy in units of m_0c^2 including the rest energy, $\theta = k_\beta T/m_0c^2$ is the characteristic dimensionless temperature, k_β is the Boltzmann constant and T is the temperature. The function K_2 denotes the modified Bessel function of the second order. Taking into account the relativistic distribution (Eq.(6)) along with the relativistic transformation coefficient A_{rel} (Eq.(5)), we have found the following expression for the relativistic RR rate coefficient in the factorized form [M.B. Trzhaskovskaya, V.K. Nikulin, R.E.H. Clark, Phys. Rev. E **78**, 035401(R) (2008)]

$$\alpha_{rel}^{(n\kappa)}(T) = < v\sigma_{rr}^{(n\kappa)} > = F_{rel}(\theta) \cdot \alpha^{(n\kappa)}(T). \quad (7)$$

Here $v = (p/E)c$ is the electron velocity with the momentum $p = \sqrt{E^2-1}$ and $\alpha^{(n\kappa)}(T)$ is similar to the recombination rate coefficient with the non-relativistic

Maxwell-Boltzmann electron distribution which may be written as

$$\alpha^{(n\kappa)}(T) = (2/\pi)^{1/2} c^{-2} (m_0 k_\beta T)^{-3/2} q_{n\kappa} \int_{\varepsilon_{n\kappa}}^{\infty} k^2 \sigma_{ph}^{(n\kappa)}(k) e^{(\varepsilon_{n\kappa}-k)/(k_\beta T)} dk. \quad (8)$$

In Eq. (7), $F_{rel}(\theta)$ is the relativistic factor which has the form

$$F_{rel}(\theta) = \sqrt{\frac{\pi}{2}\theta} \Big/ K_2(1/\theta) e^{1/\theta}. \quad (9)$$

This is just the factor which has been disregarded in all previous calculations. For example, the widely-used tables by Burgess [Mem.Roy.Astron.Soc. Pt.1 **60**, 1(1964)] of hydrogenic RR rates tabulated up to $T = \infty$ were calculated for the non-relativistic Maxwell-Boltzmann distribution or tables by Verner and Ferland based on Opacity Project [Ap. J. Suppl. **103**, 467 (1996)] calculated to $T = 10^{10}$ K and others.

The factor $F_{rel}(\theta)$ depends on temperature only. The T-dependence of the factor is demonstrated in Fig. 2. As is seen, $F_{rel}(\theta)$ differs noticeably from unity beginning with several tens of keV, that is, adopting the relativistic distribution of continuum electrons

results in a decrease of RR rates by 20% at $k_\beta T = 50$ keV and up to a factor of 7 at $k_\beta T = 1000$ keV.

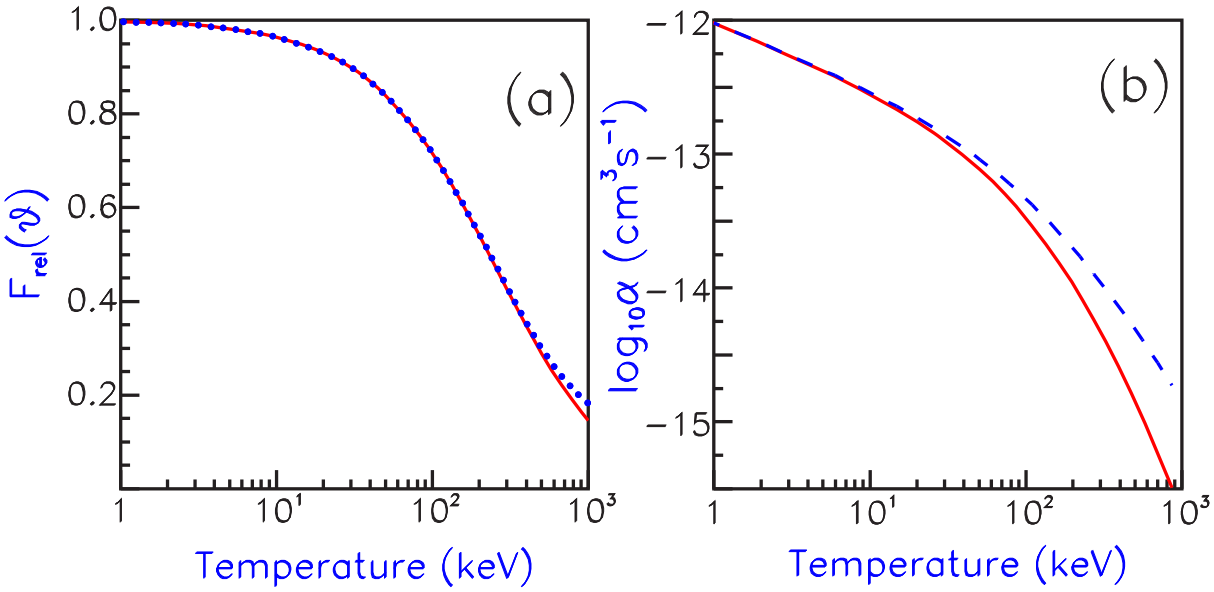

Figure 2: (a) the relativistic factor for RR and RPL rates. Solid red, the exact factor $\boldsymbol{F}_{\rm rel}(\boldsymbol{\theta})$; dotted blue, the approximate factor $\tilde{\boldsymbol{F}}_{\rm rel}(\boldsymbol{\theta})$. (b) RR rate $\boldsymbol{\alpha}^{(3s)}(\boldsymbol{T})$ with (solid red) and without (dashed blue) regard to the relativistic factor for recombination of the $\boldsymbol{3s}$ electron with the W^{64+} ion.

As is seen in Fig. 2(b), inclusion of the relativistic factor changes $\boldsymbol{\alpha}^{(3s)}(\boldsymbol{T})$ considerably at high temperatures.

To estimate the impact of non-dipole effects, we compare in Fig. 3 RRCS obtained by the DF method in the dipole approximation $\boldsymbol{\sigma}_{\rm rr}$(dip) with the exact calculation $\boldsymbol{\sigma}_{\rm rr}$(L).

Red and blue curves diverge noticeably even at several keV. The difference between them is scarcely affected by the ion charge, and the principal quantum number n_i of the shell. However, there is an essential dependence on the orbital quantum number ℓ_i.

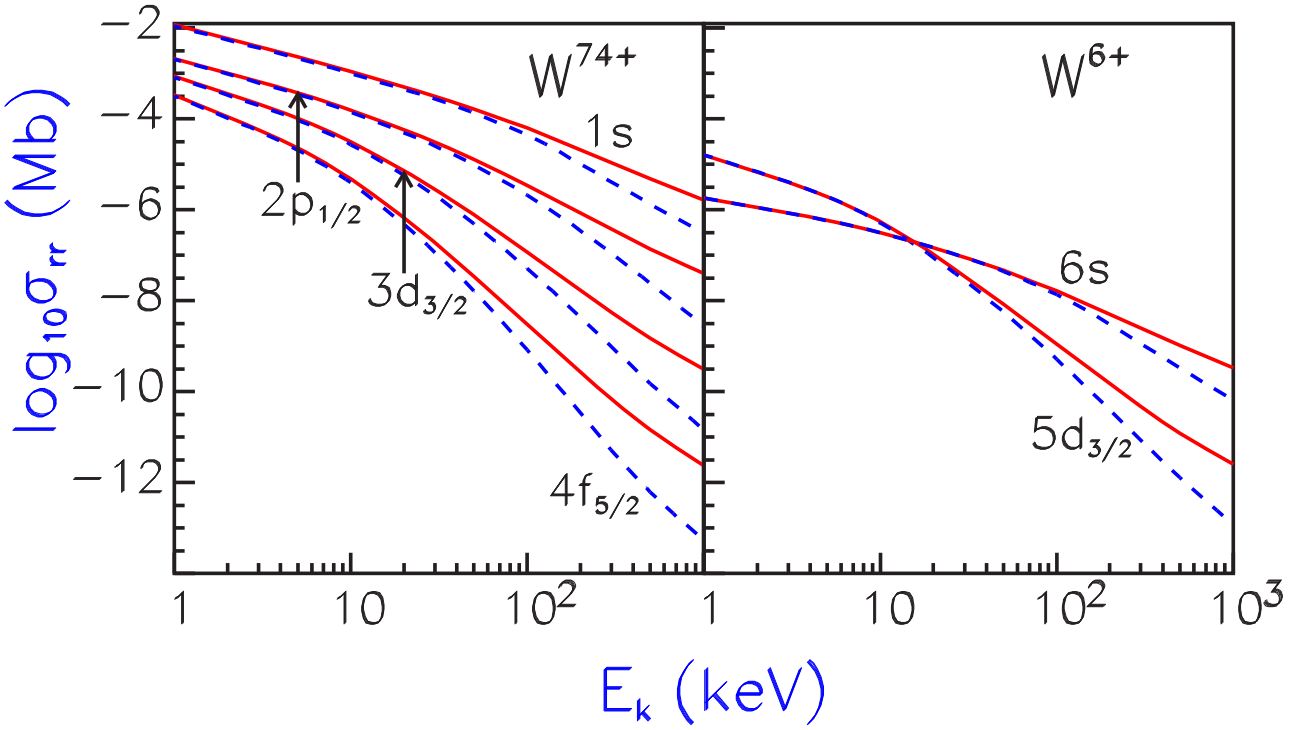

Figure 3: Subshell RRCS calculated by the DF method taking into account all multipoles L (red solid) and within the electric dipole approximation (blue dashed).

Absolute values of the difference $\Delta_{dip} = [\sigma_{rr}(L) - \sigma_{rr}(dip)]/\sigma_{rr}(L)$ in the case of the ion W^{74+} change by $8 - 18\%$ (in dependence on ℓ_i) at $E_k = 10$ keV; by $18 - 52\%$ at $E_k = 50$ keV; and by factors of $5 - 43$ at $E_k = 1000$ keV.

Table 3 shows how many multipoles L must be taken into account for various shells of the H-like ion W^{73+} at various electron energies to achieve a numerical accuracy $\sim$0.1% prescribed in our PCS calculations.

Table 3. A number of multipoles L taken into account for the W^{73+} ion.

E_k, keV	$1s$	$2p_{1/2}$	$3d_{3/2}$	$4f_{5/2}$
10	5	6	8	10
20	5	7	9	11
100	7	8	11	14
500	13	16	21	26
1000	19	24	31	37

A number of L is vastly larger than L=1 as is assumed in the dipole approximation.

The dipole approximation is also fail in calculations of RR rates at a high temperature.

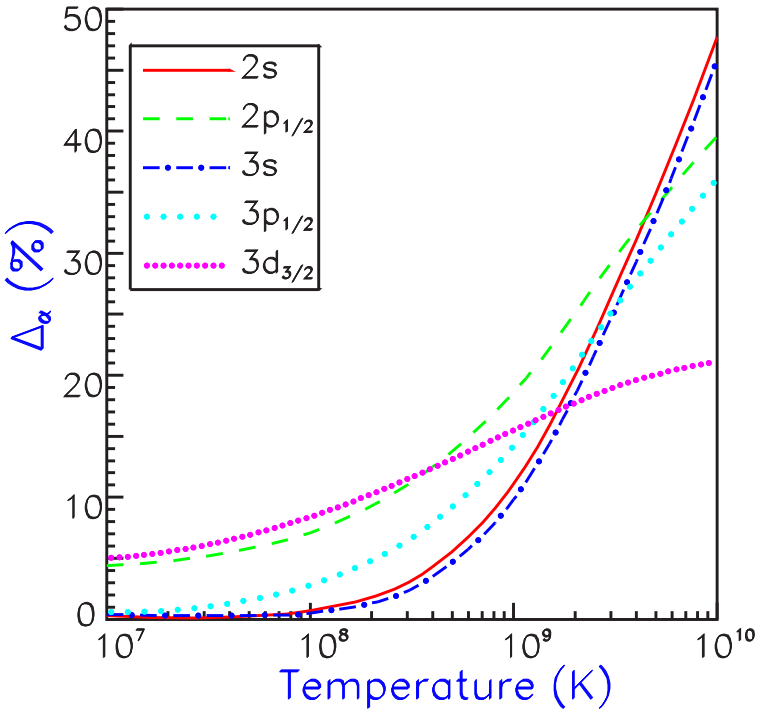

Figure 4: The difference between RR rates calculated by the DF method with regard to all multipoles and in the dipole approximation for recombination of the He-like ion W^{72+} with an electron in low states.

The inclusion of higher multipoles changes partial RR rates for W^{72+} by $\sim 7\%$ at temperature $\boldsymbol{T = 10^8}$ K, by $\sim 20\%$ at $\boldsymbol{T = 10^9}$ K, and by $\sim 50\%$ at $\boldsymbol{T = 10^{10}}$ K.

Calculations of RR and RPL rates at higher temperatures require values of RRCS/PCS at high energies. Because the proper PCS calculation at high energies is a difficult task, the PCS asymptotic tails are frequently matched. Usually the well-known asymptotic

expression derived in the framework of the NRD approximation is used

$$\sigma_{ph}^{(i)} \sim k^{-(3.5+\ell_i)}. \tag{10}$$

However, Eq. (10) breaks down for the asymptotic behavior of the relativistic PCS with regard to all multipoles L. Let us consider the product $\sigma_{ph}^{(ns)} \times k^{3.5}$ for the s-shells. If Eq.(10) holds, the product has to be a constant. In Fig. 5, the DF calculations with regard to all L (solid) and within the dipole approximation (dashed) are given.

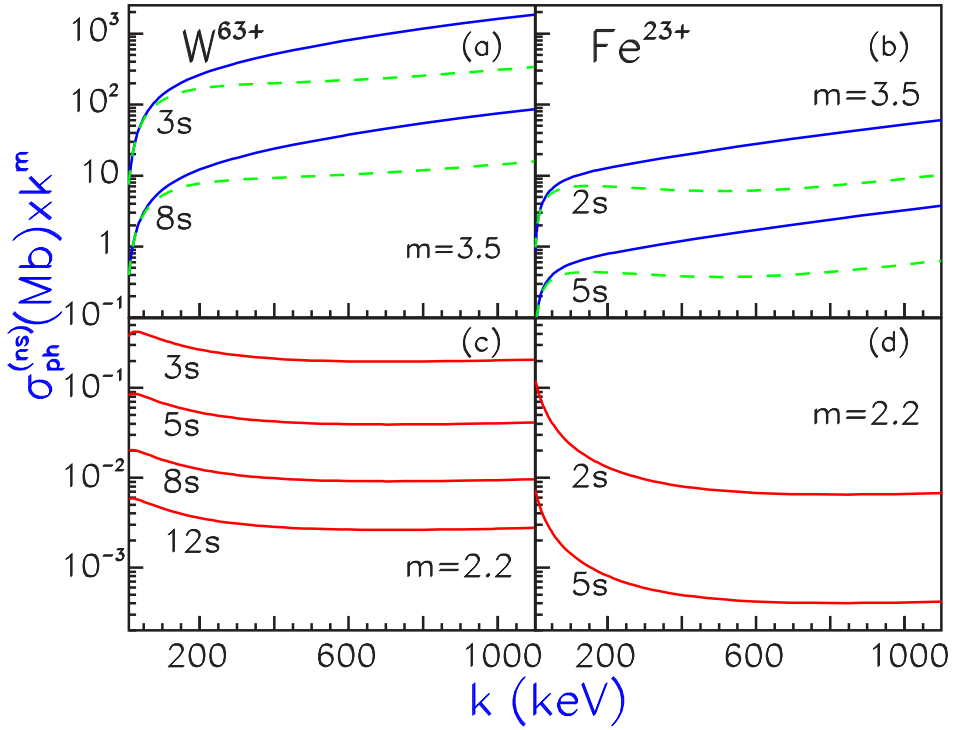

Figure 5: Product $\sigma_{ph}^{(ns)}(k) \times k^m$ with $m = 3.5$ ((a) and (b)) and $m = 2.2$ ((c) and (d)). Solid, DF calculation with regard to all multipoles L; dashed green, the DF dipole approximation.

Solid blue curves increase in the whole photon energy range at $m = 3.5$. The dashed curves are something like an approximate constant at $k \approx$ 100-150 keV. However at higher energies they increase also. We found the asymptote for the s-electrons in the relativistic multipole case

$$\sigma_{ph}^{(n\kappa)} \sim k^{-2.2}. \tag{11}$$

It should be noted that the asymptotic behavior Eq.(11) correlates well with the statement for the $1s$ shell of the hydrogen-like high-Z ions by Bethe and Salpeter who have asserted that in the relativistic case $\sigma_{ph}^{(1s)} \propto k^{-m}$ where m varies almost monotonously from $m \approx 2.7$ at energy $\approx Z^2$ Ry to $m = 1$ in the ultra-relativistic limit, never taking the value m =3.5.

However, a general expression for the PCS asymptotic behavior is unknown. So we found σ_{ph} by the direct DF calculations to several MeV for the s, p, and d shells and to several hundred keV for other shells.

4. Comparison of present calculations with previous results

Our PCS calculations are compared with results by Ichihara *et al.* for the $1s$ shell of the H-like ion W^{73+} and PCS obtained in ADAS project for the $1s$ shell of the H-like ion Xe^{53+}. The case of an one-electron ion is particularly convenient for study of the influence of non-dipole effects because the ion is free from any inter-electron interactions.

Table 4. Comparison of our PCS calculations (TNC) with results by Ichihara *et al.* [ADNDT 74, 1 (2000)] for W^{73+} and results of ADAS project [The ADAS User Manual Version 2.6. http://adas.phys.strath.ac.uk (2004)] for Xe^{53+}.

	W^{73+}, $\sigma_{\rm ph}^{(1s)}$, Mb			Xe^{53+}, $\sigma_{\rm ph}^{(1s)}$, Mb		
E_k, keV	Ichihara	TNC	E_k, keV	ADAS	TNC	Difference
0.001	9.24(-4)	9.24(-4)	0.0008	2.246(-3)	1.937(-3)	-16%
0.04	9.23(-4)	9.23(-4)	0.0397	2.240(-3)	1.935(-3)	-16%
0.4	9.13(-4)	9.13(-4)	0.3967	2.186(-3)	1.892(-3)	-16%
2	8.68(-4)	8.68(-4)	1.824	1.938(-3)	1.732(-3)	-15%
4	8.16(-4)	8.16(-4)	3.967	1.734(-3)	1.523(-3)	-14%
40	3.21(-4)	3.21(-4)	39.67	3.256(-4)	3.114(-4)	-4.5%
80	1.48(-4)	1.48(-4)	83.31	9.095(-5)	9.206(-5)	1.2%
200	3.32(-5)	3.32(-5)	182.4	1.539(-5)	1.740(-5)	12%
400	8.47(-6)	8.47(-6)	396.7	1.894(-6)	2.802(-6)	fact. 1.5
800	2.16(-6)	2.16(-6)	833.1	2.071(-7)	5.495(-7)	fact. 2.6
2000	4.34(-7)	4.34(-7)	1824	1.730(-8)	1.318(-7)	fact. 7.6
4000	1.54(-7)	1.54(-7)	3967	1.350(-9)	4.117(-8)	fact. 30
6000	8.92(-8)	8.89(-8)				

As is evident from Table 4, our calculation is in excellent agreement in the wide range of electron energy 1 eV $\leq \boldsymbol{E_k} \leq$ 6000 keV with the values from relativistic calculations by Ichihara where all multipoles were included. As a rule, our values of $\boldsymbol{\sigma}_{\rm ph}^{(\boldsymbol{n\kappa})}$ coincide with an accuracy of three significant digits given by Ichihara. The maximum difference between the two calculations is $\boldsymbol{0.3\%}$ at the highest energy $\boldsymbol{E_k} =$ 6000 keV.

On the other hand, PCS obtained within the ADAS project exceed our values by $\sim \boldsymbol{16\%}$ at low energies $\boldsymbol{E_k} \lesssim$ 4 keV and become smaller at higher energies, decreasing by a factor of ∼8 at $\boldsymbol{E_k} \approx$ 1800 keV and a factor of ∼30 at $\boldsymbol{E_k} \approx$ 4000 keV. The difference at low energies arises possible due to the influence of method of calculation while the difference at higher energies is due to a combination of ignoring the higher multipoles and adopting the semi-relativistic approximation in the ADAS calculations.

In Table 5 our values of total RR rates are compared with the only by then relativistic calculations by Kim and Pratt [Phys.Rev. A **27** 2913 (1983)] for tungsten ions W^{56+}, W^{64+}, and W^{74+}. The calculations were performed using a number of approximations, in particular, only few RRCS values were calculated by the DS method and thereafter all other necessary cross sections for each a state $\boldsymbol{n\kappa}$ were obtained by interpolation using the quantum defect method. Total RR and RPL rates were given for four values of temperature in the range 1 keV $\leq \boldsymbol{k_\beta T} \leq$ 30 keV.

Here one could hardly expect a good agreement due to the approximate approach used by Kim and Pratt. However, the comparison reveals a reasonable correlation between the two calculations. The agreement is better for the bare nucleus than for many-electron ions, probably due to the different regard to the electron exchange.

Table 5. Comparison of total RR rates $\alpha_{tot}(k_\beta T) \times 10^{12}$ (cm^3/s) obtained in the present calculations (TNC) with results by Kim and Pratt (KP).

$k_\beta T$,	W^{56+}			W^{64+}			W^{74+}		
keV	TNC	KP	$\Delta, \%$	TNC	KP	$\Delta, \%$	TNC	KP	$\Delta, \%$
1	22.8	31	–36	32.3	40	–24	84.7	94	–11
3	9.28	12	–29	13.6	16	–18	41.3	44	–6.5
10	2.95	3.5	–19	4.64	4.9	–5.6	17.4	18	–3.4
30	0.864	1.0	–16	1.48	1.4	5.4	7.08	7.3	–3.1

5. Total radiative recombination cross section

Total RRCS are determined by the capture of an electron into all states beginning

from the first open shell as follows

$$\sigma_{\rm rr}^{tot} \;=\; \sum_{n=n_{\rm min}}^{\infty} \; \sum_{\kappa=\mp 1,\mp 2,\ldots,-n} \sigma_{\rm rr}^{(n\kappa)} \;, \tag{12}$$

where $n_{\rm min}$ combined with the appropriate value of κ refers to the ground state of the recombined ion. The sum over κ has a finite number of terms which decrease rather rapidly as κ increases. The higher the energy E_k, the more rapidly the terms decrease. So for a specific value of n, all possible $2n-1$ values of κ were taken into account.

A different situation exists in summation of the infinite series over n, especially **at low electron energies**. We present in Fig. 6 relative contributions of states with various n to the total RRCS

$$B_n \;=\; \left[\sum_{\kappa} \sigma_{\rm rr}^{(n\kappa)} / \sigma_{\rm rr}^{tot}\right] \times 100\% \,. \tag{13}$$

As is seen, B_n decreases rapidly at $n \lesssim 10$ but there is no rapid convergence at higher n.

Although the contributions B_n for large n do not exceed several percent, the tails of all curves decrease very slow – the lower E_k, the slower the decrease.

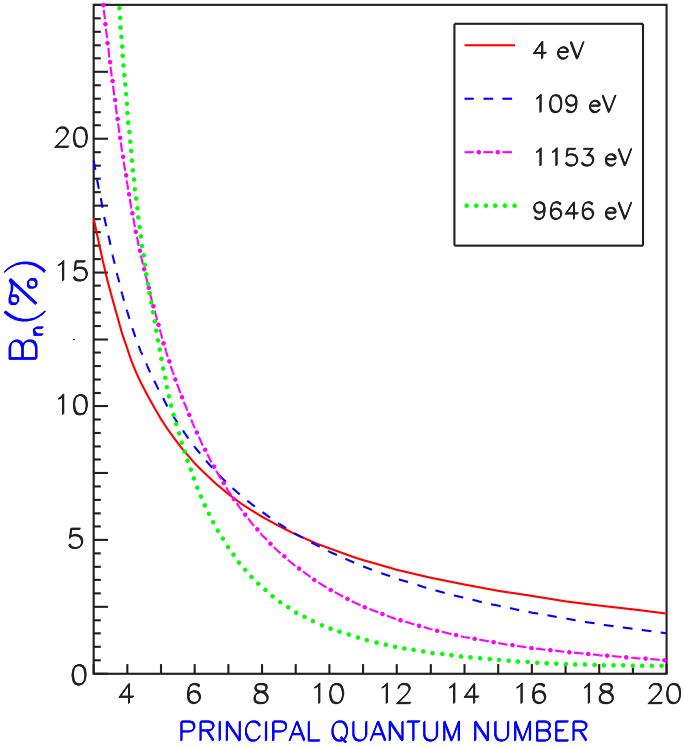

Figure 6: Convergence of the infinite series over n in the form of contributions B_n of terms $\sigma_{\rm rr}^{(n)} = \sum_\kappa \sigma_{\rm rr}^{(n\kappa)}$ to the total RRCS for the W^{64+} ion at four values of the electron energy.

In a real plasma, however, there is a cutoff of bound levels from density effects, above which recombination is not meaningful. For fusion plasmas with electron density in the range of $10^{14}/\mathrm{cm}^3$, the upper limit on the principal quantum number is $n \lesssim 20$. In our calculations, the series over n was found as a result of **summation up to $n = 20$**.

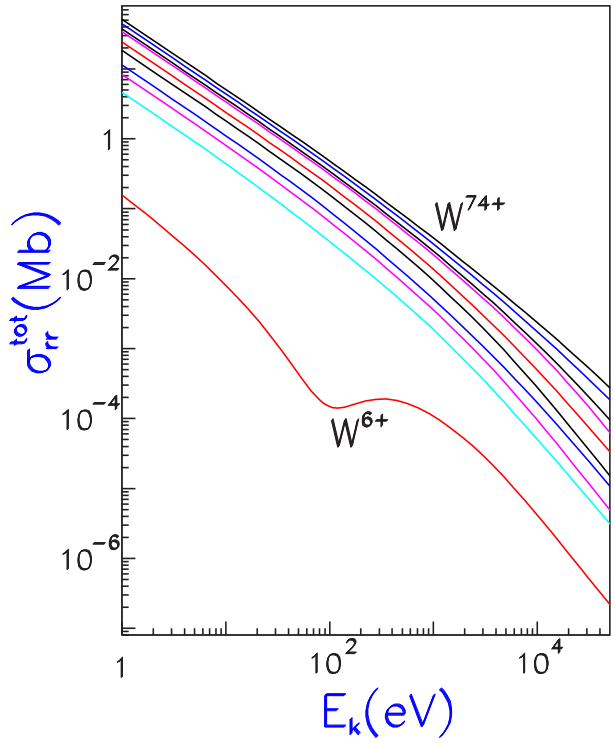

Figure 7: Total RRCS for tungsten ions from the bottom upwards: W^{6+}, W^{28+}, W^{38+}, W^{46+}, W^{56+}, W^{64+}, W^{70+}, W^{72+}, W^{73+}, and W^{74+}.

The $\boldsymbol{E_k}$-dependence of total RRCS for ten tungsten ions is shown in Fig.7. As is seen, the energy dependence $\boldsymbol{\sigma_{\rm rr}^{\rm tot}(E_k)}$ for the lowest-charged ion W^{6+} is a non-monotone function in the range $\boldsymbol{E_k} \lesssim$500 eV. This is associated with behavior of partial cross sections $\boldsymbol{\sigma_{\rm rr}^{(n\kappa)}(E_k)}$ for the lowest states. For the higher-charged ions, the $\boldsymbol{E_k}$-dependence shows up as smooth monotone curves.

6. Fitting partial photoionization cross sections

To minimize a great body of data, PCS for states with $n \leq 12$ and $\ell \leq 6$ were fitted by the analytical expression proposed in paper [D.A.Verner, D.G.Yakovlev, I.M.Band, M.B.Trzhaskovskaya, ADNDT **55**, 233 (1993)].

$$\sigma_{ph}^{(i)}(k) \;=\; \sigma_0 \left[(y-1)^2 + y_w^2\right] y^{-(5.5+\ell_i-0.5p)} \left(1+\sqrt{y/y_a}\right)^{-p}. \qquad (14)$$

Here k is the photon energy, $y = k/k_0$.

Five fit parameters $\sigma_0, k_0, y_w, y_a,$ and p were obtained by minimizing the mean-square deviation from calculated values using the simplex search method.

To assess an accuracy of the fitting procedure, we found the relative root-mean-square error δ_{av} as follows:

$$\delta_{av} \;=\; \sqrt{\frac{1}{M}\sum_{j=1}^{M}\left[\frac{\sigma_{calc}^{(i)}(k_j) - \sigma_{fit}^{(i)}(k_j)}{\sigma_{calc}^{(i)}(k_j)}\right]^2} \cdot 100\%\,, \qquad (15)$$

Usually, the fit accuracy was good with $\delta_{av} \lesssim 2\%$.

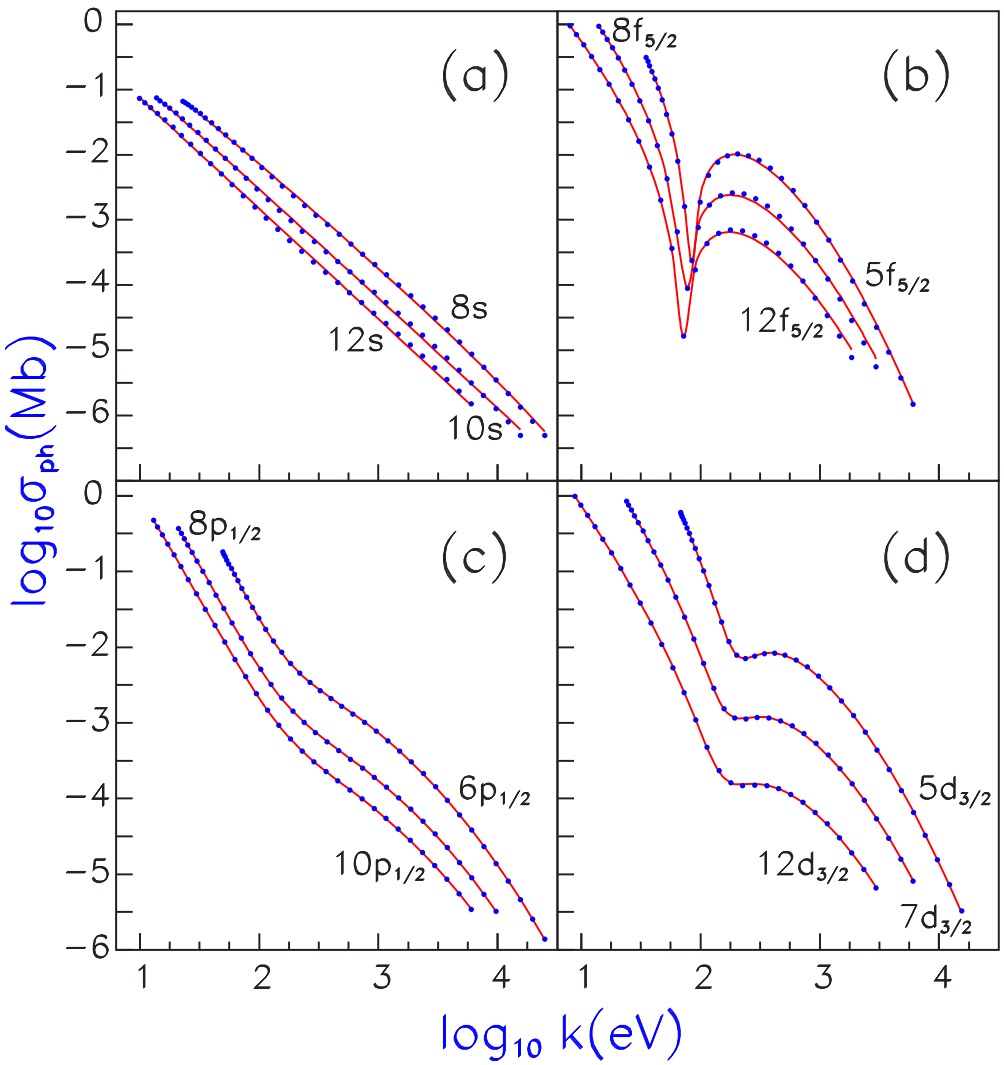

Figure 8: Fitting non-monotone PCS $\boldsymbol{\sigma}_{\boldsymbol{ph}}^{(i)}(\boldsymbol{k})$ for W^{5+}. Blue circles, calculated PCS; red curves, fitted PCS. The high $\boldsymbol{s}$ and all $\boldsymbol{f}$ states relate to the worst-fitted cases.

Fig 8 shows that even non-monotone curves $\boldsymbol{\sigma_{ph}^{(i)}(k)}$ having deep Cooper minima may be fitted quite good. Note that the high $\boldsymbol{ns}$ and $\boldsymbol{nf}$ shells of the W^{5+} ion refer to the worst-fitting cases. Nevertheless, the fitting error is small for all other shells of W^{5+}, for example, for the $\boldsymbol{np}$ shells which are not so smooth as the $\boldsymbol{ns}$ shells and for the $\boldsymbol{nd}$ shells where the Cooper minimum exists as well, but not so deep as for the $\boldsymbol{nf}$ shells. The maximum errors for the $\boldsymbol{np}$ and $\boldsymbol{nd}$ shells do not exceed $\mathbf{1.2\%}$ and $\mathbf{2\%}$, respectively. For shells with the larger orbital quantum number ($\boldsymbol{\ell > 3}$) of the lowest-charged ions as well as for all shells of the higher-charged ions, the fitting accuracy is commonly $\boldsymbol{\lesssim 1-2\%}$.

With the **five fit parameters** using Eq. (14), one can obtain the value of PCS $\boldsymbol{\sigma_{ph}^{(i)}(k)}$ per one electron at any photon energy from the energy range under consideration with an accuracy which is usually **better than $\mathbf{2\%}$**.

Recall that fifteen fit parameters were required in the earlier calculation by Clark *et al.* [R.E.H. Clark, R.D. Cowan, and F. W. Bobrowicz, ADNDT **34**, 415 (1986)], the average fitting error being less than $\mathbf{10\%}$. The associated RRCS may be easily obtained using Eq. (5).

7. Radiative recombination rate coefficients for tungsten ions

We calculated the partial and total RR rates for highly-charged ions of tungsten

from the Pd-like ion W^{28+} to the bare nucleus W^{74+}. The wide range of temperatures $\mathbf{10^3}$ K$\leq \boldsymbol{T} \leq \mathbf{10^{10}}$ K (0.09 eV $\lesssim \boldsymbol{k_\beta T} \lesssim$ 900 keV) is considered. Relativistic DF calculations were performed using expressions and methods described above. The majority of the RR rates were calculated with a numerical accuracy better than 1%, in the worst cases (outer shells and highest temperatures) the accuracy being $\lesssim \mathbf{5\%}$.

The database contains partial RR rates $\boldsymbol{\alpha_{rel}^{(n\kappa)}}$ for electron states with $\boldsymbol{n \leq 12}$ and $\boldsymbol{\ell \leq 6}$ as well as the total RR rates which are written as

$$\boldsymbol{\alpha_{tot} = \sum_{n\kappa} \alpha_{rel}^{(n\kappa)}}. \tag{16}$$

The summation in Eq. (16) was extended over all states with $\boldsymbol{n \leq 20}$. The partial rate coefficients included in the database contribute 70% - 99% into total rates.

A dependence of partial recombination rate coefficients on temperature is displayed in Fig. 9. One can see that at $\boldsymbol{T \lesssim 10^8}$ K, $\boldsymbol{\alpha^{(3p_{3/2})}}$ and $\boldsymbol{\alpha^{(3d_{5/2})}}$ are very close to each other and exceed $\boldsymbol{\alpha^{(3s)}}$ for the more inner $\boldsymbol{3s}$ shell. At $\boldsymbol{T \lesssim 10^5}$ K, $\boldsymbol{\alpha^{(4f_{7/2})}}$ and $\boldsymbol{\alpha^{(3s)}}$ have approximately the same magnitude. It is seen that $\boldsymbol{\alpha_{rel}^{(n\kappa)}}$ for shells with large $\boldsymbol{\ell}$ are at times comparable with values for shells with smaller $\boldsymbol{\ell}$ or exceed them.

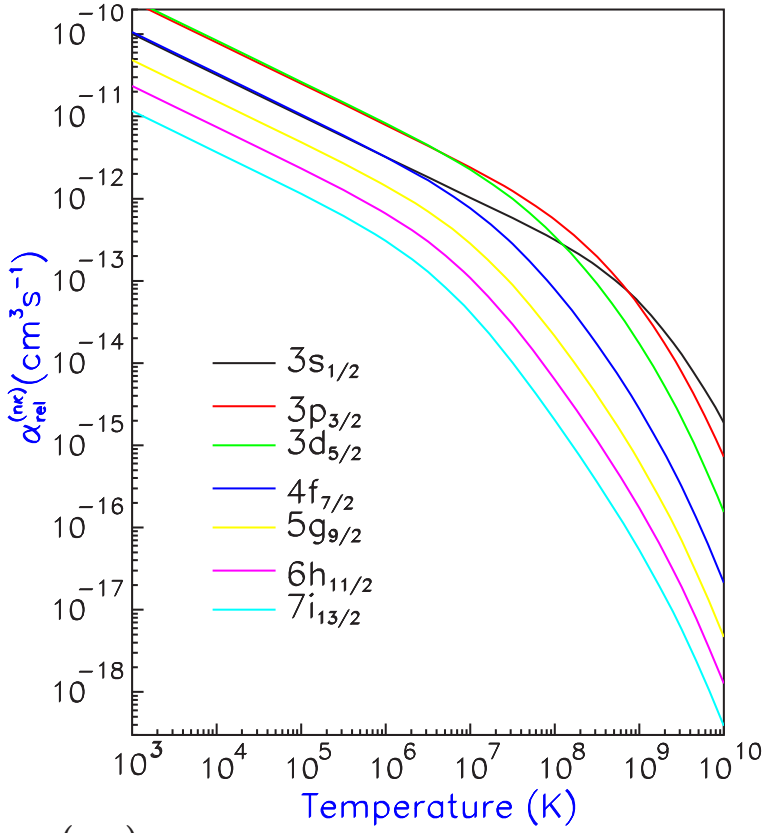

Figure 9: Partial RR rates $\boldsymbol{\alpha_{rel}^{(n\kappa)}}$ for recombination of various electrons with the ion W^{64+}.

8. Basic conclusions

• Relativistic DF calculations of partial PCS and RRCS as well as total RRCS have been performed in the electron energy range from 1 eV to 50 keV for 90 ions of sixteen elements which are of importance in fusion study including 10 tungsten ions. Partial PCS have been fitted by a simple analytical expression with five fit parameters.

• We have calculated the relativistic DF partial and total RR rates in the wide temperature range $\mathbf{10^3}$ K $\leq \boldsymbol{T} \leq \mathbf{10^{10}}$ K for nine tungsten ions which are of great current interest and for which data have not been available.

• For the first time, a new fully relativistic formula for RR rates has been derived using the relativistic Maxwell-Jüttner distribution. The formula is factorized giving rise to the temperature-dependent relativistic correction factor for which the usual expression should be multiplied. The factor changes RR and RPL rates considerably at a high energy.

• A contribution of non-dipole effects in RRCS, PCS, and RR rates has been shown to be significant (10-50%) at electron energies of the order of 10 keV and higher.

1. M.B. Trzhaskovskaya, V.K. Nikulin, and R.E.H. Clark, "*Radiative recombination and photoionization cross sections for heavy element impurities in plasma: I. Tungsten ions. Theory*". PNPI Report, PNPI-2678, 36 p. (2006).

2. M.B. Trzhaskovskaya, V.K. Nikulin, and R.E.H. Clark, "*Radiative recombination and photoionization cross sections for heavy element impurities in plasma: II. Tungsten ions. Tabulated results*". PNPI Report, PNPI-2679, 53 p. (2006).

3. M.B. Trzhaskovskaya and V.K. Nikulin, *"Comment on "Quantitative x-ray photoelectron spectroscopy: Quadrupole effects, shake up, Shirley background, and relative sensitivity factors from a database of true x-ray photoelectron spectra"*. Phys.Rev.B **75**, 177104 (2007).

4. M.B. Trzhaskovskaya, V.K. Nikulin, and R.E.H. Clark, "*Radiative recombination and photoionization cross sections for heavy element impurities in plasmas*". At. Data Nucl. Data Tables **94**, 71 (2008).

5. M.B. Trzhaskovskaya, V.K. Nikulin, R.E.H. Clark , "*Multipole and relativistic effects in radiative recombination process in hot plasmas*". Phys. Rev. E **78**, 035401 (R) (2008).

6. M.B. Trzhaskovskaya, V.K. Nikulin, and R.E.H. Clark, "*Radiative recombination rate coefficients for tungsten highly-charged ions*". At.Data Nucl.Data Tables **96**,1(2010).

9. Proposed research for tungsten ions

Our part of the present CRP is directed to elaboration of a new accurate database on RR and photoionization for tungsten ions.

- We plan to study the most important tungsten impurity ions W^{q+} in the charge ranges $24 \leq q \leq 46$ (ASDEX Upgrades) and $47 \leq q \leq 65$ (ITER).
- Relativistic calculations of partial and total RRCS and partial PCS will be performed for ground and excited states ($n \leq 20$) of the ions in the electron energy range 1 eV – 20 keV.
- A bulk of the partial PCS will be approximated by the simple analytical expressions.
- Calculations of partial and total RR rates in the temperature range 10^4 K – 10^9 K will be carried out.
- Analytical expressions for approximation of total RR rates will be deduced and the associated fit parameters will be calculated.
- Calculations of partial and total RPL rates will be performed in the temperature range 10^4 K – 10^9 K.
- The data obtained will be tabulated and published in journals ADNDT and APID as well as will be prepared for including into the IAEA electronic database ALADDIN.